# Synthesis of the $[MeAl(2\text{-}py)_3]^-$ Anion and Its Application as a Stable and Mild Pyridyl-Transfer Reagent (2-py = 2-Pyridyl)

Felipe García,[†] Alexander D. Hopkins,*[,†] Richard A. Kowenicki,[†] Mary McPartlin,[‡] Michael C. Rogers,[†] and Dominic S. Wright*[,†]

*Chemistry Department, Cambridge University, Lensfield Road, Cambridge CB2 1EW, U.K., and Department of Health and Biological Sciences, London Metropolitan University, London N7 8DB, U.K.*

*Received April 6, 2004*

The thermally stable tris(pyridyl) Al(III) complex $[MeAl(2\text{-}py)_3Li{\cdot}THF]$ (**1**·THF), obtained from the reaction of lithiopyridine [2-pyLi] with $MeAlCl_2$ (3:1 molar equiv, respectively), functions as a pyridyl-transfer reagent, as exemplified by the reaction of **1**·THF with CuCl (1:1 molar equiv), which gives the Cu(I) organometallic $[\{Cu(2\text{-}py)\}_3]_\infty$ (**2**). The solid-state structures of **1**, the dimer $[MeAl(2\text{-}py)_3Li]_2$ ($[\mathbf{1}]_2$), and **2** are reported. Complex **2**, which cannot be obtained by direct reaction of [2-pyLi] with CuCl, has a polymeric structure in which macrocyclic $[Cu(2\text{-}py)]_3$ ring units form infinite offset stacks associated by short Cu···Cu interactions between three- and four-coordinate Cu(I) centers (2.762(3) Å).



Tris(pyridyl) compounds of the general formula $[Y(2\text{-}C_5H_4N)_3]$ (Figure 1) are an important class of ligands whose coordination chemistry has been investigated extensively in the past 20 years or so.[1−4] A variety of bridgehead atoms (Y) have been incorporated into these arrangements, allowing the bite of the pyridyl-N donor centers to be tuned for specific metal coordination. The vast majority of studies so far have involved tris(pyridyl) ligands containing the lighter congeners of group 14 (Y = CH,[1] COR[2]) and group 15 (Y = N;[3] Y = P, P=O[4]). As part of our studies of main-group metal-based ligands, we became interested in the coordination chemistry of tris(pyridyl) ligands containing the heavier (most metallic) elements. In a series of studies we have reported the syntheses of a range of tris(pyridyl) ligands of this type, including the Si(IV) and Sn(IV) ligands $[Y(2\text{-}C_5H_4N)_3]$ (Y = MeSi,[5] Y = $^n$BuSn[6,7]) and the Pb(II) ligand $[Pb(2\text{-}py)_3]^-$.[8]

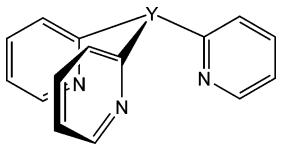


**Figure 1.** The arrangement found in tris(pyridyl) ligands.

Ligands containing more metallic bridgehead atoms coordinate *intact* to innocent metal ions such as the alkali metals. However, unlike the ligand arrangements containing C, N, and P bridgeheads, redox reactions can occur on attempted transfer of the ligands to certain transition-metal ions. For example, the reactions of $CuCl_2$ or CuCl with $[^n BuSn(2\text{-}C_5H_4N)_3LiBr]$ both result in the formation of the Cu(I) complex $[^n BuSn(2\text{-}C_5H_4N)_3CuX]$ (X = Br/Cl) (presumably as a consequence of reductive coupling of 2-pyridyl groups in the case of Cu(II)).[6] The greater lability of the 2-py groups in the more metallic ligand arrangements, although detrimental to applications in the coordination of redox-active metals, is of interest in several other respects. In particular, the possibility of obtaining stable pyridyl-transfer reagents for general applications in inorganic and organic synthesis is appealing, bearing in mind the highly thermally unstable character of alkali-metal

* To whom correspondence should be addressed. E-mail: dsw1000@cus.cam.ac.uk (D.S.W.). Fax: 01223 336362.
[†] Cambridge University.
[‡] London Metropolitan University.

(1) For examples involving CH bridgeheads, see: Keene, F. R.; Snow, M. R.; Stephenson, P. J.; Tiekink, E. R. T. *Inorg. Chem*. **1988**, *27*, 2040. Canty, A. J.; Minchin, N. J.; Skelton, B. W.; White, A. H. *Aust. J. Chem. Soc.* **1992**, *45*, 423. Lee, F. W.; Chan, M. C.-W.; Cheung, K.-K.; Che, C.-M. *J. Organomet. Chem*. **1998**, *563*, 191. Kodera, M.; Katayama, K.; Tachi, Y.; Kano, K.; Hirota, S.; Fujinami, S.; Suzuki, M. *J. Am. Chem. Soc.* **1999**, *121*, 11006. Anderson, R. A.; Astley, T.; Hitchman, M. A.; Keene, F. R.; Monbarak, B.; Murray, K. S.; Skelton, B. N.; Tiekink, E. R. T.; Toftland, H.; White, A. H. *Dalton* **2000**, 3505.

(2) For examples involving C(OR) and $C(NH_2)$ bridgeheads, see: Kanty, A. J.; Chaichit, N.; Gatehouse, B. M.; George, E. E. *Inorg. Chem*. **1981**, *20*, 4293. Keene, F. R.; Szalda, D. J.; Wilson, T. A. *Inorg. Chem*. **1987**, *26*, 2211. Jonas, R. T.; Stack, T. D. P. *Inorg. Chem*. **1998**, *37*, 6615. Brunner, H.; Maier, R. J.; Zabel, M. *Synthesis* **2001**, 2484. Arnold, P. J.; Davies, S. C.; Dilworth, J. R.; Durrant, M. C.; Griffiths, D. V.; Hughs, D. L.; Richards, R. L.; Sharpe, P. C. *Dalton* **2001**, 736.

(3) For examples involving N bridgeheads, see: Kucharski, E. S.; McWhinnie, A. H. White, W. R. *Aust. J. Chem. Soc.* **1978**, *31*, 2647. Anderson, P. A.; Keene, F. R.; Gulbis, J. M.; Tiekink, E. R. T. *Z. Kristallogr*. **1993**, *206*, 275. Mosney, K. K.; de Gala, S. R.; Crabtree, R. H. *Transition Met. Chem*. **1995**, *29*, 595. Wang, W.; Schmider, H.; Wu, Q.; Zhang, Y.-S.; Wang, S. *Inorg. Chem*. **2000**, *39*, 2397.

(4) For examples involving P and P=O bridgeheads, see: Schutte, P. R.; Rettig, S. J.; Joshi, A.; Janes, B. R. *Inorg. Chem*. **1997**, *36*, 5809. Gregorzik, R.; Wirbser, J.; Vahrenkamp, H. *Chem. Ber*. **1992**, *125*, 1575. Espinet, P.; Hernando, R.; Iturbe, G.; Villafane, F.; Orpen, A. G.; Pascual, I. *Eur. J. Inorg. Chem*. **2000**, 1031. Casares, J. A.; Espinet, P.; Martin-Alvarez, J. M.; Espino, G.; Perez-Maurique, M.; Vattier, F. *Eur. J. Inorg. Chem*. **2001**, 289.

(5) Garcia, F.; Hopkins, A. D.; Humphrey, S. M.; McPartlin, M.; Rogers, M. C.; Wright, D. S. *Dalton* **2004**, 361.

(6) Beswick, M. A.; Belle, C. J.; Davies, M. K.; Halcrow, M. A.; Raithby, P. R.; Steiner, A.; Wright, D. S. *J. Chem. Soc., Chem. Commun*. **1996**, 2619.

(7) See also: Morales, D.; Pérez, J.; Riera, L.; Riera, V.; Miguel, D. *Organometallics* **2001**, *20*, 4517.

(8) Beswick, M. A.; Davies, M. K.; Raithby, P. R.; Steiner, A.; Wright, D. S. *Organometallics* **1997**, *16*, 1109.

10.1021/om049749z CCC: $27.50 
Publication on Web 07/02/2004

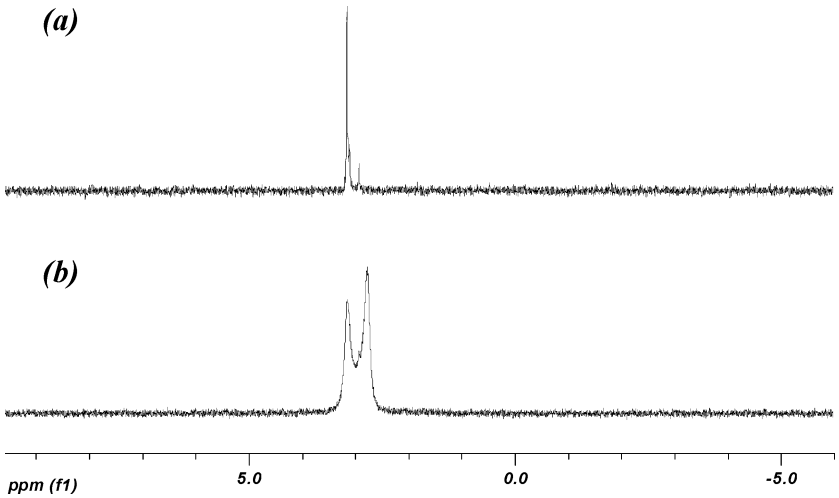


**Figure 2.** $^7$Li NMR spectra of **1**·THF in $d_8$-toluene at concentrations of (a) 0.06 mol L$^{-1}$ and (b) 0.08 mol L$^{-1}$.



reagents such as 2-lithiopyridine (whose in situ generation from 2-bromopyridine and $^n$BuLi is also restricted to THF as the solvent). Recent interest in this area has focused on pyridyl zinc reagents in organic synthesis that have greater thermal stability and conformational rigidity than their alkali-metal counterparts.[9]

We report here the synthesis and structural characterization of the tris(pyridyl) Al(III) complexes [MeAl(2-py)$_3$Li·THF] (**1**·THF) and [MeAl(2-py)$_3$Li]$_2$ ([**1**]$_2$). The ability of **1** to act as a thermally stable and soft ligand-transfer reagent for [2-py]$^-$ is illustrated in an inorganic setting by its reaction with CuCl, which gives the Cu(I) organometallic [{Cu(2-py)}$_3$]$_\infty$ (**2**). The latter cannot be obtained by reaction of CuCl with 2-lithiopyridine.

## Results and Discussion

The complex **1**·THF was prepared by the 1:3 stoichiometric reaction of $MeAlCl_2$ with a solution of 2-lithiopyridine ([2-pyLi]) in THF at −78 °C (Scheme 1 ).

**Scheme 1**

$$MeAlCl_2 + 3[2\text{-pyLi}] \xrightarrow[-2LiCl]{THF} \underset{\mathbf{1}}{[MeAl(2\text{-py})_3Li\cdot THF]}$$

After removal of the solvent under vacuum, extraction of the residue produced with toluene followed by crystallization gives **1**·THF in 48% yield (using a 50 mmol scale reaction). The complex is stable indefinitely under a nitrogen atmosphere at room temperature and is soluble in polar solvents such as THF as well as nonpolar solvents such as toluene. The room-temperature $^7$Li NMR spectrum of **1**·THF in toluene is concentration dependent. At low concentration (ca. 0.06 mol L$^{-1}$) the spectrum consists of a dominant singlet at $\delta$ 3.16, together with minor resonances at $\delta$ 3.12 and 2.94 (Figure 2a). Increasing the concentration (to ca. 0.08 mol L$^{-1}$) results in a spectrum consisting of two major resonances at $\delta$ 3.15 and 2.78 (ratio ca. 1:1.5) (Figure 2b). In the $^1$H NMR spectra of these solutions at room temperature the aromatic regions consist of a complicated series of overlapping multiplets in the regions $\delta$ 8.57−7.85 and 7.20−6.34. In addition, the two Me−Al resonances observed at low concentration (0.06 mol L$^{-1}$; $\delta$ 0.42 (s) and 0.38 (s)) are resolved into a single resonance ($\delta$ 0.39 (s)) at higher concentration (0.08 mol L$^{-1}$). At even higher concentration (ca. 0.16 mol L$^{-1}$, saturated) the room-temperature $^1$H NMR spectrum is as expected for *intact* **1**·THF, showing broad singlets for three of the aromatic protons ($\delta$ 8.44 (C(6)−H), 8.04 (C(3)−H), and 6.74 (C(4)−H)) and a sharp triplet ($\delta$ 7.16 (C(5)−H)) for the remaining aromatic proton. Although the resonance for the C(6)−H proton remains a broad singlet irrespective of the temperature (300−190 K), the other broad aromatic resonances observed at room temperature are resolved at 255 K into a doublet ($\delta$ 7.99) and triplet ($\delta$ 6.71). On the basis of these $^1$H and $^7$Li NMR spectroscopic studies and those on the dimer [**1**]$_2$ (see later), we suggest that an equilibrium between **1**·THF and the unsolvated monomer **1** (Scheme 2) is occurring in solution. As expected, the concentration of the unsolvated monomer (containing three-coordinated Li$^+$) decreases rapidly with increased concentration (over the range 0.06−0.08 mol L$^{-1}$), since solvation of the Li$^+$ cation in **1**·THF (containing four-coordinate Li$^+$) is highly favorable. This solvation is clearly favored over the aggregation of unsolvated **1** into dimers [**1**]$_2$, which

**Scheme 2**

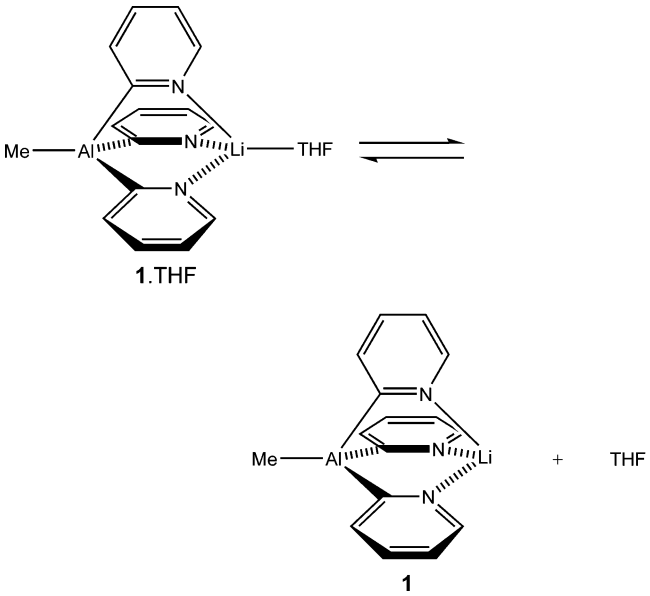


(9) For example, see: Alami, M.; Peyrat, J.-F.; Belachmi, L.; Brion, J.-D. *Eur. J. Org. Chem.* **2001**, 4207.

**Scheme 3**

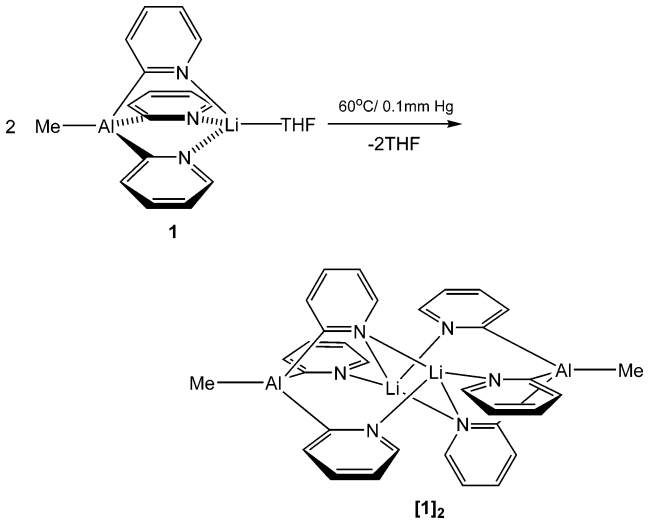


are not observed in NMR spectroscopic studies of **1**·THF at any concentration. The stability of the unsolvated monomer at low concentration may conceivably rely on an ion−dipole interaction with the toluene solvent. Unfortunately, the presence of an equilibrium between **1** and **1**·THF could not be confirmed by cryoscopic molecular mass measurements, owing to the low solubility of **1**·THF in benzene.

Placing **1**·THF under vacuum for ca. 16 h at 60 °C followed by recrystallizing from toluene gives the unsolvated complex $[MeAl(2\text{-py})_3Li]_2$ ($[\mathbf{1}]_2$) (Scheme 3). Like **1**·THF, the $^7$Li NMR and $^1$H NMR spectra of $[\mathbf{1}]_2$ are concentration dependent. The room-temperature $^7$Li NMR spectrum of $[\mathbf{1}]_2$ in toluene at low concentration (ca. 0.04 mol $L^{-1}$) shows two singlets at $\delta$ 3.36 and 3.18 (Figure 3a). The latter resonance has a chemical shift very similar to the dominant resonance found in solutions of **1**·THF at low concentration, and we therefore assign this to the monomer $[MeAl(2\text{-py})_3Li]$ (**1**). At high concentration (ca. 0.07 mol $L^{-1}$) the spectrum consists of one major singlet at $\delta$ 3.36, with the resonance at $\delta$ 3.18 being observed as a broad shoulder (Figure 3b) (which can be resolved into a separate singlet at 290 K). The room-temperature $^1$H NMR spectra at low and high concentrations show a complicated pattern of overlapping resonances in the aromatic region ($\delta$ 8.46−7.80 and 7.20−6.34), consistent with the existence of more than one solution species. Two Me−Al resonances are observed at $\delta$ 0.42 and 0.37, the former growing with increased concentration. We assign the resonance at $\delta$ 0.42 and the associated $^7$Li resonance at $\delta$ 3.36 to the *intact* dimer $[\mathbf{1}]_2$, a species which (as would be expected) is not found for **1**·THF at low concentration. It therefore appears that the solution process observed for $[\mathbf{1}]_2$ in toluene involves a monomer/dimer equilibrium between **1** and $[\mathbf{1}]_2$. Like **1**·THF, the low solubility of $[\mathbf{1}]_2$ in benzene prevented cryoscopic molecular mass measurements on this compound.

The Cu(I) organometallic $[\{Cu(2\text{-py})\}_3]$ (**2**) is obtained in 64% yield as bright orange needles from the 1:1 stoichiometric reaction of **1**·THF with CuCl in toluene (Scheme 4). Attempts to prepare **2** by the direct reaction

**Scheme 4**

$$\underset{\mathbf{1}\cdot\mathrm{THF}}{[MeAl(2\text{-py})_3Li\cdot THF]} \xrightarrow[CuCl]{\text{toluene}} {}^1/_3[\{Cu(2\text{-py})\}_3] + \underset{\mathbf{2}}{[MeAl(2\text{-py})_2ClLi]}$$

of 2-lithiopyridine with CuCl in THF at −78 °C resulted in very rapid decomposition into Cu metal, presumably via disproportionation of Cu(I) into Cu(0) and Cu(II) (possibly also accompanied by a Cu(II)-mediated coupling reaction of the $[Al(2\text{-py})_3]^-$ anion to give 2,2′-bipyridine[10]). Compound **2** was basically characterized by elemental analysis and $^1$H NMR spectroscopy prior to obtaining its solid-state structure.

The low-temperature (180 K) X-ray structures of **1**·THF, $[\mathbf{1}]_2$, and **2** were obtained. Details of the data collections and refinements are listed in Table 1. Key bond lengths and angles for compounds **1**·THF, $[\mathbf{1}]_2$, and **2** are listed in the figure captions to Figures 4−6, respectively.

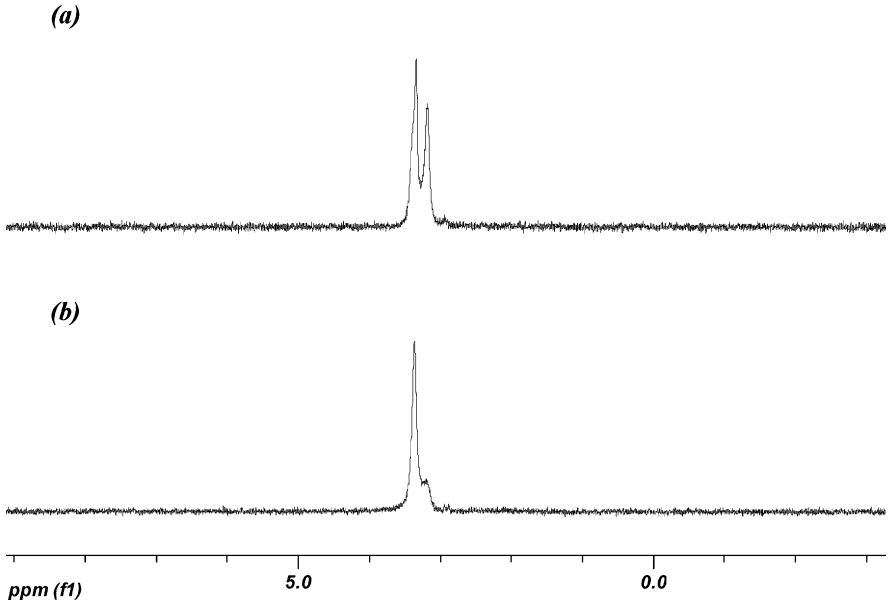


**Figure 3.** $^7$Li NMR spectra of $[\mathbf{1}]_2$ in $d_8$-toluene at concentrations of (a) 0.04 mol $L^{-1}$ and (b) 0.07 mol $L^{-1}$.

**Table 1. Crystal Data and Structure Refinement Details for 1·THF, [1]$_2$, and 2[a]**

| | **1**·THF | [**1**]$_2$ | **2** |
|---|---|---|---|
| empirical formula | $C_{20}H_{23}AlLi\text{-}N_3O$ | $C_{32}H_{30}Al_2N_6$ | $C_{15}H_{12}Cu_3N_3$ |
| fw | 355.33 | 566.46 | 424.90 |
| cryst syst | triclinic | monoclinic | tetragonal |
| space group | $P\bar{1}$ | $P2_1/n$ | $P4/ncc$ |
| $a$ (Å) | 8.7990(18) | 8.9730(18) | 20.506(3) |
| $b$ (Å) | 9.761(2) | 10.458(2) | |
| $c$ (Å) | 12.690(3) | 16.807(3) | 7.0245(14) |
| α (deg) | 76.84(3) | | |
| $\beta$ (deg) | 71.93(3) | 97.25(3) | |
| $\gamma$ (deg) | 75.70(3) | | |
| $Z$ | 2 | 2 | 8 |
| $V$ (Å$^3$) | 990.5(3) | 1574.0(5) | 2953.8(8) |
| $\rho$(calcd) (Mg m$^{-3}$) | 1.191 | 1.215 | 1.911 |
| $\mu$(Mo Kα) (mm$^{-1}$) | 0.114 | 0.125 | 4.273 |
| $F$(000) | 376 | 592 | 1680 |
| no. of rflns collected | 9594 | 11 855 | 9154 |
| cryst size (mm) | 0.28 × 0.07 × 0.07 | 0.10 × 0.10 × 0.10 | 0.37 × 0.30 × 0.12 |
| $\theta$ range (deg) | 3.60−27.54 | 3.10−27.46 | 3.65−27.46 |
| no. of indep rflns ($R_{int}$) | 4594 (0.050) | 3530 (0.105) | 9154 (0.049) |
| abs cor | | semiempirical from equivalents | |
| max, min transmissn | 1.006, 0.885 | 0.880, 0.760 | 0.628, 0.559 |
| no. of data/restraints/params | 4508/0/284 | 3530/0/234 | 1694/0/96 |
| goodness of fit on $F^2$ | 1.063 | 1.009 | 1.047 |
| $R$ indices ($I > 2\sigma(I)$) | | | |
| R1 | 0.058 | 0.060 | 0.034 |
| wR2 | 0.112 | 0.120 | 0.059 |
| R indices (all data) | | | |
| R1 | 0.094 | 0.129 | 0.058 |
| wR2 | 0.131 | 0.146 | 0.067 |
| largest peak and hole(e Å$^{-3}$) | 0.231, −0.273 | 0.270, −0.303 | 0.458, −0.399 |

[a] Data in common: $T$ = 180(2) K; $\lambda$ = 0.710 73 Å.



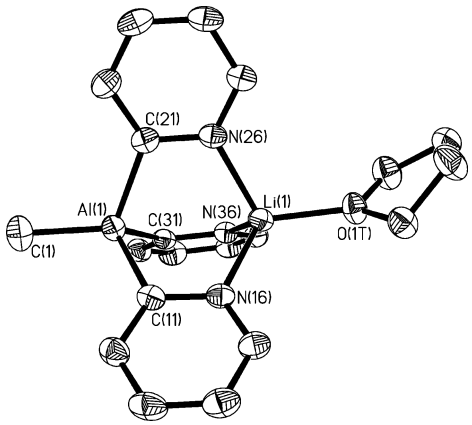


**Figure 4.** Structure of the tris(pyridyl) Al(III) complex **1**·THF. Thermal ellipsoids are drawn at the 40% probability level. H atoms have been omitted for clarity. Selected bond lengths (Å) and angles (deg): Al(1)−C(1) = 1.980(3), Al(1)−C(11,21,31) range 2.021(2)−2.027(2), N(16,26,36)−Li(1) range 2.045(4)−2.056(4), Li(1)−O(1T) = 1.941(4); C(1)−Al(1)−C(11,21,31) range 112.2(1)−115.96(1), C(11)−Al(1)−C(21) = 104.4(1), C(11)−Al(1)−C(31) = 103.90(9), C(21)−Al(1)−C(31) = 103.83(9), Al−C$_\alpha$−N(16,26,36) range 114.4(2)−116.7(2).

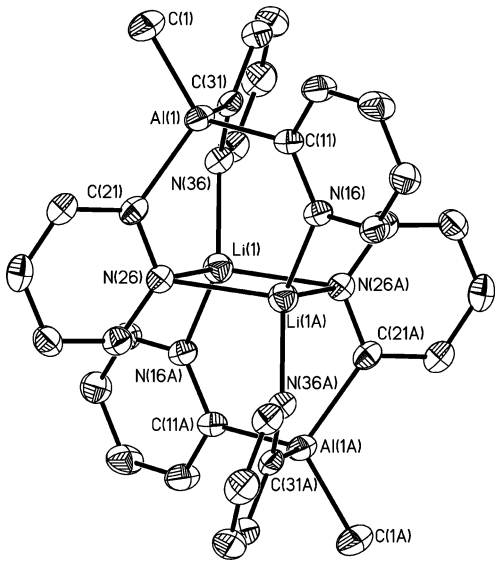


**Figure 5.** Structure of the unsolvated dimer [**1**]$_2$. Thermal ellipsoids are drawn at the 40% probability level. H atoms have been omitted for clarity. Selected bond lengths (Å) and angles (deg): Al(1)−C(1) = 1.982(3), Al(1)−C(11,21,31) range 2.010(3)−2.025(3), N(16)−Li(1A) = 2.007(5), N(26)−Li(1) = 2.139(4), N(26)−Li(1A) = 2.232(5), N(36)−Li(1) = 2.015(5); C(1)−Al(1)−C(11,21,31) range 108.6(1)−112.5(1), C(11)−Al(1)−C(21) = 104.7(1), C(11)−Al(1)−C(31) = 112.4(1), C(21)−Al(1)−C(31) = 107.8(1), Al−C$_\alpha$−N(16,26,36) range 119.7(2)−120.6(2), Li(1)−N(26)−Li(1A) = 72.0(2), N(26)−Li(1)−N(26A) = 108.0(2). Symmetry transformations used to generate equivalent atoms A: $-x$, $-y + 1$, $-z$.

The compound **1**·THF has the expected structure, consisting of a [MeAl(2-py)$_3$]$^-$ anion which coordinates a monosolvated Li$^+$ cation using the three pyridyl-N centers (Figure 4). The structural arrangement is therefore similar to that found in the group 14 Li$^+$ complexes [$^n$BuSn(2-py)$_3$LiBr][6] and [MeSi(2-py)$_3$LiX] (X = Cl/Br),[5] although the latter contain neutral tris-(pyridyl) ligand arrangements. In theory, the bites of [RE(2-py)$_3$]$^{x-}$ ligands should be dependent largely on two geometric factors: (i) the C−E bond lengths and (ii) the C−E−C bond angles. For neutral group 14 ligands of this type (E = C, Si, Sn; $x$ = 0) the dominant factor is the C−E bond length. Although the bridgehead C−E−C angle decreases on going from C (ca. 111°)[1,2] to Si (ca. 106°)[5] to Sn (ca. 101°),[6,7] the increase in C−E

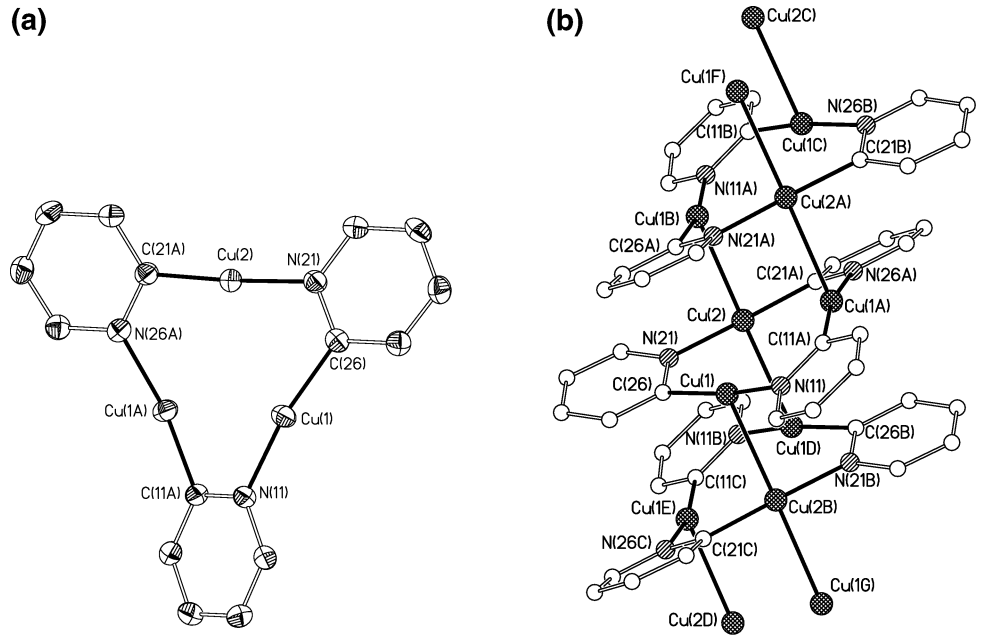


**Figure 6.** (a) Ortep drawing of one trimeric ring in **2** (thermal ellipsoids are drawn at the 40% probability level). In the solid state the ring is disordered and has crystallographic $C_2$ symmetry about an axis through Cu(2) and the midpoint of the N(11)−C(11A)/C(11)−N(11A) vector. (b) Association of the trimeric units via Cu···Cu interactions to give stacks running parallel to the *c* axis. Adjacent trimeric units within each "stack" are related by crystallographic inversion symmetry. H atoms have been omitted for clarity. Selected bond lengths (Å) and angles (deg): Cu(1)−N(11)/C(11A) = 1.900(3), Cu(1)−N(26) = 1.901(3), Cu(2)−N(21,21A) = 1.898(3), intertrimer Cu···Cu = 2.7624(6); N(11)/C(11A)−Cu(1)−N(26) = 168.0(1), Cu(2B)···Cu(1)−N(11)/C(11A) = 93.42(9), Cu(2B)···Cu(1)−N(26) = 97.18(8), mean N(21)−Cu(2)−C(21A) = 176.6(2), Cu(1D)···Cu(2)···Cu(1B) = 175.49(3), Cu(1D)···Cu(2)−N(21) = 89.77(8), Cu(1D)···Cu(2)−C(21A) = 90.37(8). Symmetry transformations used to generate equivalent atoms: (A) $-x, -y, -z + 1$; (B) $-y, -x, -z + {}^1/_2$; (C) $y, x, z - {}^1/_2$.



bond lengths results in a net increase in the ligand bite (defined by the mean N···N distance, from ca. 2.9−3.0 Å for C,[1,2] to ca. 3.1 Å for Si,[5] to ca. 3.21 Å for Sn[6,7]). In contrast, the large bite of the $[MeAl(2\text{-}py)_3]^-$ anion of **1** appears to stem from a combination of the large C−Al−C bridgehead angles (range 103.83(9)−104.4(1)°) and relatively long C−Al bonds (range 1.980(3)−2.022(2) Å). The result is a ligand bite (mean N···N 3.23 Å) which is close to that observed for the neutral $[^n BuSn(2\text{-}py)_3]$ ligand.[6,7]

The structure of the unsolvated complex $[\mathbf{1}]_2$ is that of the centrosymmetric dimer $[MeAl(2\text{-}py)_3Li]_2$ (Figure 5). Two of the 2-py groups of each of the $[MeAl(2\text{-}py)_3]^-$ anions are involved in terminal N−Al bonding to the $Li^+$ cations within the central $N_2Li_2$ core of the complex (N(6)−Li(1) = 2.015(5) Å, N(16)−Li(1A) = 2.007(5) Å), while the remaining 2-py group is responsible for the association of the $[MeAl(2\text{-}py)_3Li]$ units into a dimeric arrangement. The ($sp^2$ hybridized) py-N atoms of these ligands $\mu_2$ bridge the $Li^+$ cations within the central $Li_2N_2$ core of $[\mathbf{1}]_2$ (N(26)−Li(1) = 2.130(4) Å, N(26)−Li(1A) = 2.232(5) Å). Comparison of the metric parameters for the $[MeAl(2\text{-}py)_3]^-$ anions in **1**·THF and $[\mathbf{1}]_2$ reveals that, although the bond lengths in both complexes are almost identical within crystallographic errors, the major difference is found in the distorted nature of the anion in $[\mathbf{1}]_2$. In particular, a large expansion of the C(11)−Al(1)−C(36) angle (112.39(1)°) results from the two associated 2-py rings coordinating the two $Li^+$ cations on either side of the $Li_2N_2$ ring unit (cf. 104.7(1) and 107.8(1)° for the other two C−Al−C angles within the anion). The increase in ligand bite required in order to coordinate the $Li^+$ cations of the core of $[\mathbf{1}]_2$ (N···N range 3.43−4.52 Å; cf. mean 3.23 Å in **1**·THF) is also aided by the expansion of the Al−$C_\alpha$−N angles (mean 115.4° in **1**·THF, mean 120.2° in $[\mathbf{1}]_2$). Although the coordination of metal dications ($M^{2+}$) by tris(pyridyl) ligands (L) in complex cations of the type $[L_2M]^{2+}$ is a well-known structural class,[1−4] the coordination of monocations into a dimeric arrangement such as $[\mathbf{1}]_2$ is (to our knowledge) unique for this class of ligands. To our knowledge, the $[MeAl(2\text{-}py)_3]^-$ anion found in **1**·THF and $[\mathbf{1}]_2$ is the first tris(pyridyl) ligand of its type for a metallic group 13 element.[11a] In fact, there appear to have been *no* pyridyl complexes of any type for any metallic group 13 elements structurally characterized previously.[11b]

The structure of the ligand transfer product **2** consists of macrocylic $[Cu(2\text{-}py)]_3$ units which, in the crystal, show $C_2$ symmetry (with the $C_2$ axis through Cu(2) and the midpoint of the N(11)−C(11A)/C(11)−N(11A) bond) (Figure 6a). This is the result of disorder in the solid state, in which the site of N(11) is 50% occupied by C(11) (and similarily for the symmetry-generated site C(11A)/N(11A)). Consistent with this disorder, in the second pyridyl ring the sites of N(21) and C(26) are 50% occupied by C(21) and N(26), respectively. The trimeric constituents of **2** are constructed from the association of three [(2-py)Cu] units to give a ring of virtual $C_3$ symmetry shown in Figure 6a; the trimeric units are

(10) It is known that 2-lithiopyridine undergoes oxidative coupling in the presence of Cu(II), giving bipyridine and Cu(I); see: Partks, J. E.; Wagner, B. E.; Holm, R. H. *J. Organomet. Chem.* **1973**, *56*, 53.

(11) (a) The closest relatives to **1** and **2** are N−Al-bonded (1,4-dihyropyrid-1-yl)aluminum complexes; see: Nensen, K.; Lemke, A.; Strumpf, T.; Bolte, M.; Fleischer, H.; Pulham, C.; Gould, R. O.; Harris, S. *Inorg. Chem.* **1999**, *38*, 4700. (b) Pyridyl boron compounds are known; for example: Weiss, W.; Pritzkow, H.; Siebert, W. *Eur. J. Inorg. Chem.* **1999**, 363.

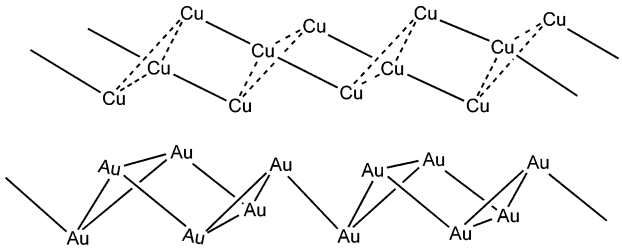


**Figure 7.** Comparison of the association of the $Cu_3$ units in **2** with that observed in the Au analogue.

randomly distributed throughout the crystal in two orientations. A similar situation occurs in the structure of the Au(I) analogue [{Au(2-py)}$_3$]$_\infty$, in which again all N and C donor atoms within the $(AuNC)_3$ ring units are disordered.[12b] In the trimeric units of **2**, the three 2-py ring units adopt a propeller-like conformation with respect to the $[Cu(NC)]_3$ core with the nine Cu, N, and C atoms of the ring being coplanar to within 0.24 Å. Association of the $[Cu(2\text{-py})]_3$ units occurs within the lattice to form infinite columns via closed-shell Cu···Cu interactions (2.7624(6) Å, Figure 6b), resulting in an unusual square-planar geometry for Cu(2) and T-shaped geometries for Cu(1) and Cu(1A). The Cu···Cu interactions in **2** are within the range of values observed previously in Cu(I) compounds.[13a] However, the presence of intermolecular Cu···Cu interactions in **2** (which are not supported by bridging ligands) is rare, an example being the trinuclear Cu(I) complex [{Cu(2-(3(5)-pz)py)}$_3$] (2-(3(5)-pz)py = 2-[3(5)-pyrazolyl]pyridine), in which trimeric ring units are associated by unsupported intermolecular Cu···Cu interactions into loosely linked dimers (2.905(3) Å).[13b] The additional possibility of significant $\pi$-arene···Cu and/or N···Cu interactions reinforcing the association of the trimers of **2** is unlikely, bearing in mind the lengths of the intermolecular contacts involved (i.e., N(26A)···Cu(1) = 3.76 Å (with the distance between the centroid of the associated 2-py ring and Cu(1) being 3.61 Å)).

The aggregation of the units of **2** is related to that found in [{Au(2-py)}$_3$]$_\infty$,[12b,14] in which [{Au(2-py)}$_3$]$_2$ dimers are associated by two Au···Au interactions, which then aggregate into a steplike polymer via a single (rather than double) Au···Au interaction (Figure 7). Unlike **2**, the Au analogue also contains discrete dimers that do not associate further into a polymeric arrangement. A key influence on the different modes of aggregation observed in **2** and its Au analogue is the relative strengths of Cu···Cu and Au···Au closed-shell interactions. Au···Au interactions of this type are significantly stronger than Cu···Cu interactions.[15] In **2**, the intramolecular Cu···Cu distances within the $[Cu(2\text{-py})]_3$ units (Cu···Cu = 3.13−3.16 Å) are at the higher end of the range of values expected for Cu···Cu closed-shell interactions.[13a] In contrast, the Au···Au distances in the $[Au(2\text{-py})]_3$ units of the Au analogue suggest significant intramolecular bonding (3.309(2)−3.346(3) Å). Thus, although the intermolecular connectivities found in the polymers or discrete dimer units of [{Au(2-py)}$_3$]$_\infty$ are lower than in **2**, this is more than made up for by intramolecular metal···metal interactions. A noteworthy feature of **2** is seen in a view of the lattice down the crystallographic *c* axis in Figure 8. The packing of polymers of **2** results in the formation of cylindrical channels that are bounded by four "stacks". These channels are ca. 6.5 Å in diameter.

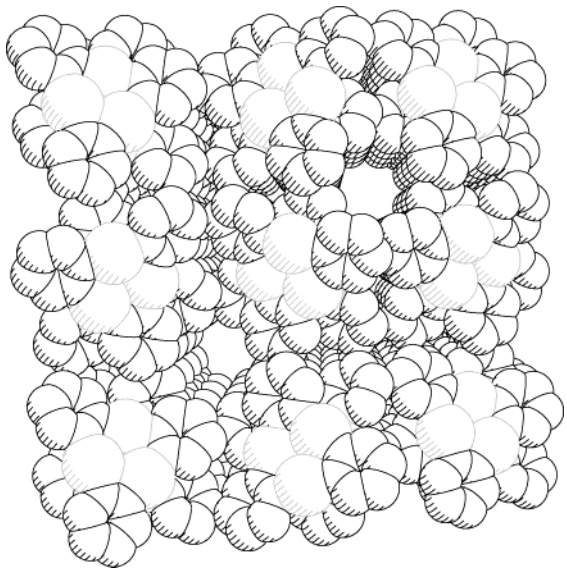

**Figure 8.** Section of the lattice of **2** viewed down the $C_4$ axis, showing the formation of cylindrical channels bounded by bundles of four columns of $[Cu(2\text{-py})]_3$ stacks.

## Conclusions

The results reported in this paper show that the first group 13 pyridyl complexes containing the [MeAl(2-py)$_3$]$^-$ anion are readily prepared and are stable at room temperature. The reaction of this anion with CuCl illustrates the potentially broad applications of the [MeAl(2-py)$_3$]$^-$ anion as a stable and soft source of the 2-py ligand.

## Experimental Section

Compounds **1,** [**1**]$_2$, and **2** are air- and moisture sensitive and were prepared under dry, $O_2$-free $N_2$ on a vacuum line. 2-Bromopyridine was distilled over $CaH_2$ and stored over molecular sieves prior to use. $^n$BuLi, $MeAlCl_2$, and CuCl were supplied commercially (Aldrich). Compounds **1**·THF, [**1**]$_2$, and **2** were isolated and characterized with the aid of an $N_2$–filled glovebox fitted with a Belle Technology $O_2$ and $H_2O$ internal recirculation system. Melting points were determined using a conventional apparatus and sealing samples in capillaries under $N_2$. IR spectra were recorded as Nujol mulls using NaCl plates and were run on a Perkin-Elmer Paragon 1000 FTIR spectrophotometer. Elemental analyses were performed by first sealing the samples under $N_2$ in airtight aluminum boats (1−2 mg), and C, H, and N content was analyzed using an Exeter Analytical CE-440. $^1$H and $^7$Li NMR spectra were

(12) (a) Vaughan, L. G. J. *Am. Chem. Soc.* **1970**, *92*, 730. (b) Hayahi, A.; Olmstead, M. M.; Attar. A.; Balch, A. L. *J. Am. Chem. Soc.* **2002**, *124*, 5791.

(13) (a) Conquest software for searching the Cambridge Structural Data Base and Visualizing Crystal Structures (Jan 2004): Bruno, I. J.; Cole, J. C.; Edgington, P. R.; Kessler, M.; Macrae, C. F.; McCabe, P.; Pearson, J.; Taylor, R. *Acta Crystallogr.* **2001**, *B58*, 389. Values of 2.35−3.58 Å (mean 2.752 Å) have been reported in a variety of Cu complexes. (b) Singh, R.; Long, J. R.; Stravropoulos, P. *J. Am. Chem. Soc.* **1997**, *119*, 2942.

(14) For other examples of trinuclear Cu(I) complexes, see: Aalten, H. L.; van Koten, G.; Goubitz, K.; Stam, C. H. *J. Chem. Soc., Chem. Commun.* **1985**, 1252. Doyle, G.; Eriksen, K. A.; van Engen, D. K. *J. Am. Chem. Soc.* **1986**, *108*, 445. Kang, H. C.; Do, Y.; Knobler, C. B.; Hawthorne, M. F. *J. Am. Chem. Soc.* **1987**, *109*, 6530. Niemeyer, N. *Organometallics* **1998**, *17*, 4649.

(15) Pyykkö, P. *Chem. Rev.* **1997**, *97*, 597.

recorded on a Bruker ATM DRX500 spectrometer, in dry $d_8$-toluene or $d_8$-THF (using the solvent resonances as internal reference standards for $^1$H NMR and external standards of 85% $H_3PO_4/D_2O$ for $^{31}$P and a saturated solution of $LiCl/D_2O$ for $^7$Li NMR spectra).

**Synthesis of 1·THF.** A solution of 2-pyLi was prepared by the dropwise addition of $^n$BuLi (31.25 mL, 1.6 mol $L^{-1}$ in hexanes, 50 mmol) to a solution of 2-bromopyridine ([2-Brpy]; 4.75 mL, 50 mmol) in THF (120 mL). The mixture was stirred for 3 h at −78 °C before $MeAlCl_2$ (16.7 mL, 1.0 mol $L^{-1}$ in hexane, 16.7 mmol) was added dropwise. The reaction mixture was warmed to room temperature, and the solvent was removed under vacuum to give a brown solid. Toluene (80 mL) was added and the mixture stirred (8 h) and then filtered. The filtrate was reduced in volume under vacuum until a precipitate formed. The precipitate was dissolved by the addition of THF (ca. 5 mL). Storage at −15 °C (24 h) gave light brown crystals of **1**·THF. Yield: 2.85 g (48%). IR (Nujol, NaCl; $\nu$/cm$^{-1}$): 3040 (w) (C−H aryl), 1577 (s), 1549 (s) (C···N str). $^1$H NMR (500.2 MHz, 25 °C, $d_8$-toluene, 0.16 mol $L^{-1}$): $\delta$ 8.44 (br s, 3H, C(6)−H), 8.04 (br s, 3H, C(3)−H), 7.16 (t, 5 Hz, 3H, C(5)−H) and 6.74 (br s, 3H, C(4)−H), 3.67 (mult, 4H, $-CH_2O$, THF), 1.51 (mult, 4H, $-CH_2-$, THF), 0.37 (s., 3H, Me−Al). $^7$Li NMR (194.40 MHz, 25 °C, rel saturated solution of LiCl/$D_2O$): $\delta$ 3.16 (s), 3.12 (s), and 2.94 (s) (ca. 0.06 mol $L^{-1}$); $\delta$ 3.15 and 2.78 (ratio ca. 1:1.5) (ca. 0.08 mol $L^{-1}$). Anal. Found: C, 66.2; H, 6.5; N, 11.5. Calcd for **1**·THF: C, 67.6; H, 6.5; N, 11.8.

**Synthesis of [1]$_2$. 1**·THF (0.355 g, 1.0 mmol) was placed under vacuum (0.1 mm Hg) for ca. 16 h at 60 °C in an oil bath. The solid was then dissolved in toluene (10 mL) and filtered to remove a small amount of insoluble material. Storage at 25 °C (24 h) gave [**1**]$_2$ as colorless blocks. Yield (first batch, crystals): 0.068 g (19%). Decomposes to a black solid at >200 °C. IR (NaCl, Nujol Mull; $\nu$/cm$^{-1}$): 3060 (m) (C−H sryl), 1583 (s), 1551 (s) (C···N str.). $^1$H NMR (500.2 MHz, 25 °C, $d_8$-toluene): $\delta$ 8.47−6.35 (collection of overlapping mult, total 12H, 2-py), 0.42 (s), 0.38 (s) (total 3H, Me−Al). $^7$Li NMR (194.40 MHz, 25 °C, rel saturated solution of $LiCl/D_2O$): $\delta$ 3.36 (s), 3.18 (s) (ca. 0.04 mol $L^{-1}$); $\delta$ 3.36 (major), 3.18 (minor, shoulder) (ca. 0.07 mol $L^{-1}$). Anal. Found: C, 67.7; H, 5.4; N, 14.8. Calcd for [**1**]$_2$: C, 67.8; H, 5.3; N, 14.8.

**Synthesis of 2. 1**·THF (0.355 g, 1.0 mmol) was dissolved in toluene (20 mL) before addition of solid CuCl (0.036 g, 0.36 mmol). The mixture was stirred at room temperature (16 h) to give a golden yellow solution that was filtered through Celite to remove a small quantity of powder. The filtrate was reduced in volume under vacuum until precipitation commenced. The solid was gently heated until it dissolved. Storage at room temperature (16 h) gave long, golden orange needles of **2**. Yield: 0.03 g (64% based on Cu supplied). $^1$H NMR (500 MHz, 25 °C, $d_8$-THF): $\delta$ 8.60−6.89 (collection of overlapping mult, C−H, 2-py). Anal. Found: C, 40.6; H, 2.8; N, 9.3. Calcd for **2**: C, 42.4; H, 2.8; N, 9.9. The reaction of **1**·THF with 3 equiv of CuCl in toluene led to decomposition, apparently into Cu metal. Similarly, the direct reaction of 2-pyLi with CuCl (1:1 equiv in THF at −78 °C for ca. 3 h) resulted in a large amount of decomposition into Cu metal, and none of **2** could be isolated from the filtrate despite repeated attempts. It can be noted that although the stability of CuCl is well-known to be solvent dependent, a suspension of CuCl alone in THF is stable under these reaction conditions.

**Crystal Structures of 1·THF, [1]$_2$, and 2.** Crystals of **1**, [**1**]$_2$, and **2** were mounted directly from solution under argon using an inert oil which protects them from atmospheric oxygen and moisture. X-ray intensity data were collected using a Nonius Kappa CCD diffractometer. Details of the data collections and structural refinements are given in Table 1. The structures were solved by direct methods and refined by full-matrix least squares on $F^2$.[16] In **1** the aromatic hydrogens were directly located with the hydrogens on C(1) and the THF solvent molecule included in idealized positions. In [**1**]$_2$ the aromatic hydrogens were directly located and the methyl hydrogens on C(1) were included in idealized positions. The structure of **2** exhibited crystallographic disorder, which has been discussed above. For the pyridyl ring containing N(11)/C(11) the disorder was dictated by symmetry. For the pyridyl ring containing N(21) and ortho-C(26) the disorder was modeled to give a $[Cu(2\text{-py})]_3$ unit with virtual $C_3$ symmetry. Evidence for this came from the anisotropic displacement parameters of N(21)/C(21) and C(26)/N(26) and the reduction in R1 ($I > 2\sigma(I)$) by 0.024 from 0.361 to 0.337. All hydrogens in **2** were included in idealized positions. Atomic coordinates, bond lengths and angles, and thermal parameters for **1**, [**1**]$_2$, and **2** have been deposited with the Cambridge Crystallographic Data Centre.

**Acknowledgment.** We gratefully acknowledge the EPSRC (F.G., M.M., M.C.R., D.S.W.), Churchill and Fitzwilliam Colleges Cambridge (Fellowship for A.D.H.), the Cambridge European Trust (F.G.), and The States of Guernsey and The Domestic and Millenium Fund (R.A.K.) for financial support. We also thank Dr. J. E. Davies for collecting X-ray data for **1** and **2**.

**Supporting Information Available:** Full listings of X-ray crystallographic data, atomic coordinates, thermal parameters, bond distances, bond angles and hydrogen parameters for **1**·THF, [**1**]$_2$, and **2**; these data are also available as CIF files. This material is available free of charge via the Internet at http://pubs.acs.org.

OM049749Z

(16) Sheldrick, G. M. SHELX-97; University of Göttingen, Göttingen, Germany, 1997.